

---

ARTICLE

---

## Induced activity in tungsten as an ADSS target

Maitreyee Nandy\*

Saha Institute of Nuclear Physics, 1/AF, Bidhannagar, Kolkata 70006, India

High neutron yield from thick tungsten target presents it as a possible target for accelerator driven subcritical system (ADSS) if the problem of cooling can be mitigated. Generation of induced radioactivity in an ADSS target impose some restrictions on the operational parameters. In this work we have estimated induced radioactivity in a thick tungsten target by 1 mA proton beam at 400 MeV, 800 MeV and 1.2 GeV. Theoretical simulation has been carried out using the code QMD. In a thick target projectile interaction is considered from the incident energy down to reaction threshold. Hence at lower energies, upto 200 MeV, ALICE-91 is used to calculate the excitation functions. After 30 days of continuous operation, maximum activity  $\sim 4 \times 10^7$  MBq is produced for  $^{170}\text{Lu}$ .  $^3\text{H}$  activity is of the order of  $3 \times 10^5$  MBq.

**Keywords:** *accelerator driven subcritical system; tungsten; induced activity; QMD; saturation activity*

### 1. Introduction

A part of India's total electricity production is achieved from nuclear industry amounting to  $\sim 3000$  MU per year during the last few years. The PHWR and BWR commissioned for the purpose employ U as the fuel and the spent fuel contains a large amount of transuranic (TRU) elements and actinides. Disposal of these long-lived high level wastes is a problem to the nuclear industry. Safe operation of the power reactors at near criticality is another problem to be mitigated. Accelerator driven sub-critical system (ADSS) has emerged as one of the preferred solutions to tackle both these problems. ADSS acts as a source of spallation neutrons which are supplied to the reactor core to sustain the fission chain reaction as well as for transmutation of long-lived isotopes. The neutronics of the system should ensure a hard neutron spectrum with high neutron yield, low yield of chemical and radio-toxicity, satisfying at the same time several other operational criteria [1]. This mandates a careful selection of the ADSS target. Different materials have been studied for their suitability to be used as ADSS target. Lead and lead-bismuth alloys have proved to be good choices for the purpose [2]. Of the other materials uranium and tungsten have high neutron yields [3] required for ADSS. Tungsten may be used as an ADSS target because besides having high cross section of neutron production it has low probability for production actinides by neutron capture [4]. In this work we have estimated the radioactivity produced in the tungsten target due to reactions induced by the primary proton beam at 400 MeV, 800 MeV and 1.2 GeV and by the secondary neutrons produced thereof.

### 2. Method of calculation

#### 2.1. Radioactivity induced by proton beam

ADSS employs thick target so that the full beam energy is used for neutron production. This results in a high neutron yield which may in turn be utilised for transmutation of long-lived wastes. In our work we have considered a thick tungsten (W) target. W has five naturally occurring isotopes,  $^{184}\text{W}$ ,  $^{186}\text{W}$ ,  $^{182}\text{W}$ ,  $^{183}\text{W}$  and  $^{180}\text{W}$  with natural abundances of 30.64%, 28.43%, 26.50%, 14.13% and 0.12%, respectively. In a thick target the projectile interacts at gradually degrading energies. In order to take this into account excitation functions of the product nuclides due to reactions induced in each of the five W isotopes are calculated over the energy range from incident energy to the threshold of reaction [5]. Yield of a radionuclide from a target isotope at a given projectile energy is determined from the excitation function considering attenuation of projectile flux inside the target. The total yield for the particular nuclide is then calculated by summing the yields of the product nuclide from a target isotope over the entire projectile energy range and then computing the weighted sum for all the naturally occurring isotopes of the target. Attenuation of the projectile flux inside the target is calculated using the program SRIM [6].

The induced activity  $A_i$  of a radionuclide 'i' at the end of an irradiation period  $t_i$  is given by [7],

$$A_i = \sum_j \int_{E_{th}}^{E_0} N_j(E) \sigma_j(E) \phi(E) (1 - e^{-\lambda_i t_i}) dE \quad (1)$$

where  $N_j(E)$  = number of target atoms in j-th isotope available for interaction at energy E

$\sigma_j(E)$  = production cross section of the nuclide 'i'

---

\*Corresponding author. Email: maitreyee.nandy@saha.ac.in

$\phi_j(E)$  = projectile flux

$\lambda$  = decay constant of the radionuclide

The saturation activity is given by,

$$A_i^s = \sum_j \int_{E_{th}}^{E_0} N(E) \sigma(E) \phi(E) dE \quad (2)$$

## 2.2. Radioactivity induced by secondary neutrons

Energy distribution of neutron yield from a thick target is calculated from the production cross section of neutrons in a target isotope over the entire interaction energy range for the incident projectile beam. Excitation function of a radionuclide due to neutron induced reaction is then folded with thick target neutron yield to obtain the yield the radionuclide.

## 2.3. Nuclear reaction models:

The excitation functions of the radionuclides are calculated using two nuclear reaction model codes Quantum Molecular Dynamics (QMD) due to Niita et al [8,9] and ALICE-91 [10]. QMD has originally been developed to calculate heavy ion reaction cross sections, but was later modified for nucleon induced reactions. The code has been designed to work at projectile energies from 400 MeV to a few GeV. As the projectile interaction is considered from the incident energy down to the reaction threshold, at the lower energies ALICE-91 has been used to estimate the nuclide production cross section.

### 2.3.1. Quantum molecular dynamics (QMD) model

The QMD code has been described in the original work as well as our earlier works. For the sake of completeness we give a very brief description of the code and input parameters.

The code QMD employs Monte Carlo simulation of quantum molecular dynamics (QMD) approach to calculate the emission cross sections for direct (DIR) and preequilibrium (PEQ) emissions. This is followed by a statistical decay model to calculate the evaporation cross section from the composite nucleus<sup>4-6</sup>. In this work we have carried out QMD calculations for 10000 histories, 1 fm/c time step with 7 fm maximum impact parameter.

### 2.3.2 ALICE-91

ALICE-91 is a well known and widely used code due to M. Blann<sup>1</sup>. It calculates pre-compound emission cross section in the framework of hybrid /geometry-dependent hybrid (GDH) model and compound nuclear or equilibrium emission cross section using Weisskopf-Ewing formalism. In the GDH version of the hybrid model effect of longer mean free path and limitation in hole energy at the nuclear surface have been taken into account. In the present work we have used optical model subroutine to calculate the cross-section of the reverse reaction channel. Fermi gas

level density formalism, with level density parameter  $a = A/9$ , has been considered for residual nuclei where  $A$  is the mass number of the nucleus.

## 3. Results and discussion

We have estimated the induced activity in a thick tungsten target for an ADSS due to 400 MeV, 800 MeV and 1.2 GeV proton induced reactions and due to reactions induced by secondary neutrons. In **Figures 1, 2** and **3** we have shown the activity induced in the target, after 30 days of irradiation, for  $^3\text{H}$  and isotopes of elements with atomic number  $Z=69-75$  (i.e. ) by proton beam with incident energies of 0.4, 0.8 and 1.2 GeV, respectively. These product isotopes range have been chosen because highest amount of activity is induced for these nuclides which constitutes the mass range close to target nuclides and projectile-like fragment.

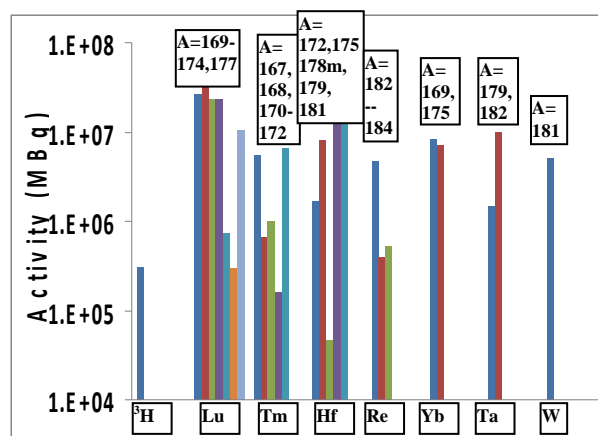


Figure 1. Induced activity of the nuclides by 0.4 GeV, 1 mA incident proton beam.

From Figure 1 we see that activity of  $^3\text{H}$  is  $3 \times 10^5$  MBq. Maximum activity is produced for  $^{170}\text{Lu}$  and is of the order of  $4 \times 10^7$  MBq.  $^{170}\text{Lu}$  decays by electron capture with a half life of 2 days. It has 1.28 and 2.04 MeV gamma rays. Several other isotopes of Lu, e.g.,  $^{169,171,172,177}\text{Lu}$  and  $^{179,181}\text{Hf}$  also builds up an activity  $\sim 10^7$  MBq. Most of these nuclides decay by electron capture with half-lives of a few days. They have characteristic  $\gamma$ -emission at 0.96 and 1.45 MeV for  $^{169}\text{Lu}$ , 0.67 and 0.74 MeV for  $^{171}\text{Lu}$ , 0.9 and 1.09 MeV for  $^{172}\text{Lu}$ .  $^{179}\text{Hf}$  decays by internal transition with emission of 0.122, 0.362 and 0.453 MeV gamma rays.

These should be guarded against external exposure during target handling after irradiation.  $^{177}\text{Lu}$  and  $^{181}\text{Hf}$  are  $\beta^-$  emitter with a half lives of 6.7 days (considered for our calculation) and 42.39 days, respectively. But  $^{177\text{m}}\text{Lu}$  has a half life of 160.4 days which could not be differentiated in this work. Proper precaution should be taken against internal contamination for  $^{177}\text{Lu}$  and  $^{181}\text{Hf}$ .

Among the other nuclides produced  $^{167,172}\text{Tm}$ ,  $^{169,175}\text{Yb}$ ,  $^{172,175}\text{Hf}$ ,  $^{179,182}\text{Ta}$ ,  $^{181}\text{W}$  and  $^{182}\text{Re}$  are produced

with activities of  $\sim 10^6$  MBq. Activities of other nuclides produced range between  $5 \times 10^4$  MBq to  $5 \times 10^5$  MBq.  $^{172}\text{Tm}$ ,  $^{175}\text{Yb}$  and  $^{182}\text{Ta}$  are  $\beta^-$  emitters and they decay to stable products. In 30 days irradiation saturation activity is reached for  $^{172}\text{Tm}$ ,  $^{169,170}\text{Lu}$  and  $^{182}\text{Re}$ .

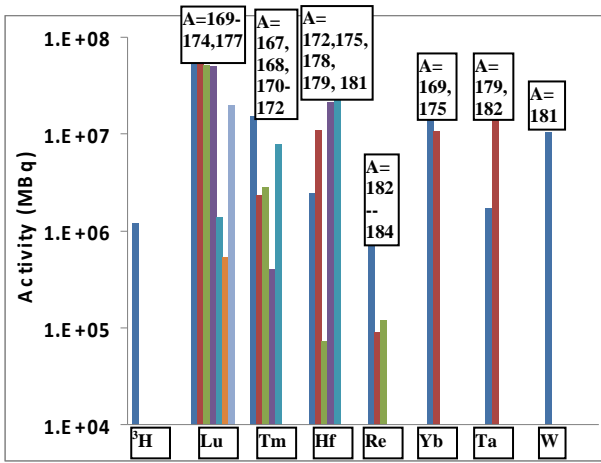


Figure 2. Induced activity of the nuclides by 0.8 GeV, 1 mA incident proton beam.

From Figure 2, it has been observed that at 0.8 GeV incident energy activity build up for all isotopes of Yb, Lu, Hf, Ta and W increases while that for Tm and Re isotopes decreases compared to activity induced at 0.4 GeV. From Figure 3 we see that activity of Re and Ta isotopes increases compared to that for 0.8 GeV proton energy.

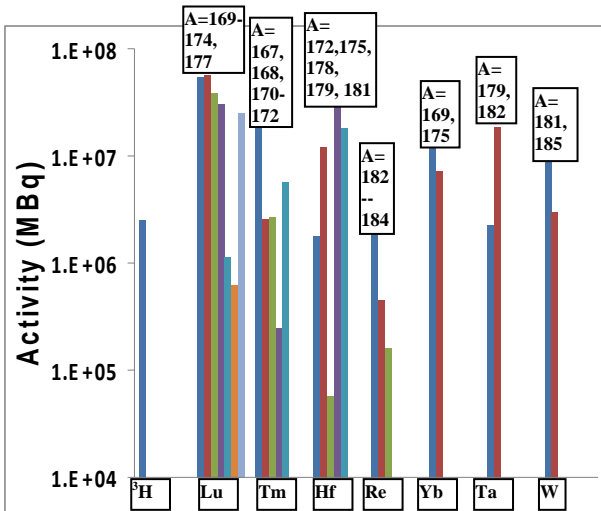


Figure 3. Induced activity of the nuclides by 1.2 GeV, 1 mA incident proton beam.

Comparison of Figures 1, 2 and 3 shows that activity of  $^3\text{H}$  produced in the reaction system for 30 days of irradiation increases from  $3 \times 10^5$  MBq at 0.4 GeV to  $2 \times 10^6$  MBq at 1.2 GeV. In Figure 4 we have shown the activity build up profile for  $^3\text{H}$  at beam energies of 0.4 – 1.2 GeV for 1 – 30 days of irradiation.  $^3\text{H}$  through ground water contamination acts as a biologically hazardous radionuclide. Careful monitoring for  $^3\text{H}$  production and its spread should be carried out to ensure

protection against its contamination

In Figure 5 we have shown the induced activity profile for some light nuclides in the beam energy range of 0.4 – 1.2 GeV after 30 days of irradiation.  $^{32}\text{P}$ ,  $^{39}\text{Ar}$ ,  $^{46}\text{Sc}$ ,  $^{59}\text{Fe}$  are  $\beta^-$  emitters while  $^{24}\text{Na}$ ,  $^{49}\text{V}$ ,  $^{51}\text{Cr}$ ,  $^{54}\text{Mn}$  are  $\beta^+$  emitters. Half lives of these nuclides range between several days to few hundred years. Precaution must be taken against internal contamination and spread of activity to the environment from these nuclides.

Our study showed that for the same input power production of  $^3\text{H}$  at 0.4 GeV proton energy is approximately one order of magnitude lower than that at 1.2 GeV. But yield of target-like and intermediate mass fragments are more at lower energies when operated at same beam power.

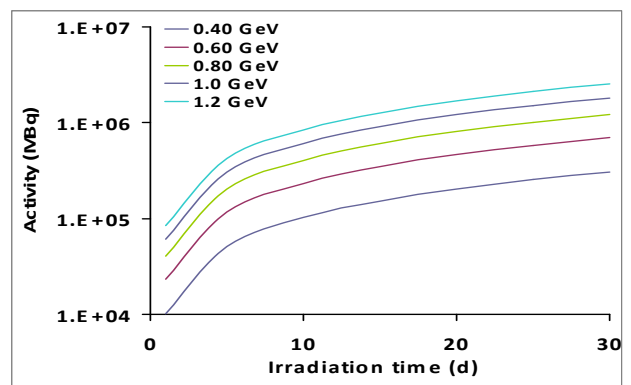


Figure 4. Induced activity build up of  $^3\text{H}$  with time at different beam energies and 1 mA beam current.

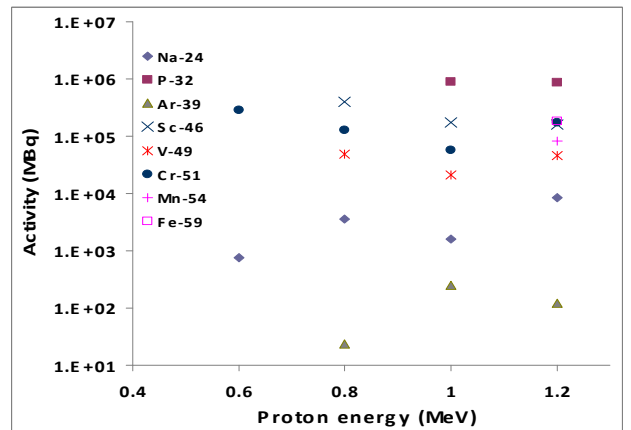


Figure 5. Induced activity profile of some light nuclides vs beam energy for 1 mA beam current after 30 days of irradiation.

In Table 1 we have shown the activity build up of some heavy nuclides due to secondary neutrons at 0.4, 0.8 and 1.2 GeV proton energy. At 1.2 GeV proton energy most of the total neutron yield is obtained for neutron energies upto 0.6 GeV. At the two lower energies this limit is 0.4 and 0.25 GeV, respectively. From Table 1 we observe that due to neutron induced

reaction several  $\beta^-$  emitters are produced with activities of the order of  $10^5 - 10^6$  MBq. These are  $^{182,183,184}\text{Ta}$ ,  $^{180,181}\text{Hf}$ .

Table 1. Radioactivity induced by the secondary neutrons after 30 days of irradiation by 1 mA proton beam.

Radio-nuclide	Half life	Activity (MBq) at beam energy (GeV)		
		0.4	0.8	1.2
$^{181}\text{W}$	121.2d	$5 \times 10^6$	$7.2 \times 10^6$	$8.4 \times 10^6$
$^{184}\text{Ta}$	8.7d	$2 \times 10^5$	$4.3 \times 10^5$	$6 \times 10^5$
$^{183}\text{Ta}$	5.1d	$4.7 \times 10^6$	$5.8 \times 10^6$	--
$^{182}\text{Ta}$	114.4d	$6 \times 10^6$	$9 \times 10^6$	$2 \times 10^7$
$^{181}\text{Hf}$	42.4d	$4 \times 10^6$	$5 \times 10^6$	$7.5 \times 10^6$
$^{180}\text{Hf}$	5.5h	$6.2 \times 10^6$	$7 \times 10^6$	$7.6 \times 10^6$
$^{179}\text{Hf}$	25.0d	$7.1 \times 10^6$	$8 \times 10^6$	$1.1 \times 10^7$

Induced activity of various radionuclides reported in this work is generated through theoretical simulation only, using two nuclear reaction model codes. Comparison of the present results with those from similar works would have been an interesting study. But though induced activity produced in W target by electron beam has widely been studied, data on proton beam induced activity are scarce. D. Ene [11] estimated inclusive radioactivity generation by proton projectile at 2.5 GeV in W with 20% by weight of NaK inside for European Spallation Source. Khandaker et al [12] measured yield of some product radionuclides at 40 MeV while Dimitriev [13] studied the generation of induced radioactivity at energies upto 22 MeV. As none of these works deals with the energy range studied in this work, a comparative study could not be carried out.

#### 4. Conclusion

Our study on induced radioactivity in W, used as an ADSS target, by the primary proton beam and by the secondary neutrons produced in the thick target shows that activities of the order of  $10^6 - 10^7$  MBq are produced for several  $\beta$  and  $\gamma$ -emitting radioisotopes after irradiation for 30 days by 1 mA beam. Comparison with our earlier works [14, 15] shows the activity induced for  $^3\text{H}$  is of the similar magnitude as that in the case of Pb or LBE targets. Our calculations produce a negligible amount of total  $\alpha$ -activity which is not of concern. Amount of TRU and actinides produced is also small. This shows that once the heat load of the target can be handled, W, which is used as an ADSS target in electron accelerators [16], may be used as an ADSS target in a proton beam also.

In estimating the radioactivity induced by the secondary neutrons in the target, we have assumed an isotropic distribution of neutron yield in the thick target. This is an approximation—in the energy range used for this study high energy neutrons will have forward peaked angular distribution. Nevertheless, in our case the assumption of isotropic distribution does not introduce appreciable deviation from the actual scenario.

The reason for this is two-fold – firstly, we are calculating the total activity induced by the neutrons in the thick W target which is not influenced by the directional distribution of the neutrons. Secondly about 83% of the total fast neutron yield (neutron energy above 1 MeV) is contributed by neutrons with energy between 1-20 MeV and among these 71% are produced from statistical decay of the fast fragments. These neutrons do not show strong angular anisotropy.

#### Acknowledgements

The author wishes to thank Dr. P. K. Sarkar, Head, Health Physics Division, Bhabha Atomic Research Centre, Mumbai, India for helpful discussions.

#### References

- [1] J. Zhang, N. Li, *J. Nucl. Mat.* 326 (2004), pp. 201-210.
- [2] T. Obara, T. Miura and H. Sekimoto, *Prog. Nucl. Energy* 47 (2005), pp. 577- 585.
- [3] W. P. Swanson, *Health Phys.* 37 (1979), pp. 347-335.
- [4] P. M. Swaney, *Target and Core Optimization for an Electron Accelerator-Driven Transmutation* (Thesis), North Carolina State University (2007).
- [5] M. Nandy and P. K. Sarkar, *Nucl. Instrum. Methods A* 583 (2007), pp. 248-255.
- [6] J.F. Ziegler, J.P. Biersack and U. Littmark, *The Stopping and Range of Ions in Solids*, Pergamon Press, New York, (1985).
- [7] M. Nandy, T. Bandyopadhyay and P.K. Sarkar, *Phys. Rev. C* 63 (2001), 034610.
- [8] K. Niita, S. Chiba, T. Maruyama, T. Maruyama, H. Takada, T. Fukahori, Y. Nakahara and A. Iwamoto, *Phys. Rev. C* 52, (1995) pp. 2620-2635 .
- [9] K. Niita, T. Maruyama, T. Maruyama and A. Iwamoto, *Prog. Theor. Phys.* 98 (1997), pp. 87-94.
- [10] M. Blann, *Lawrence Livermore National Laboratory Report UCID 19614*, (1982); M. Blann, ICTP Workshop Report no. SMR/284-1, (1988).
- [11] D. Ene, [http://www.stralsakerhetsmyndigheten.se/Global/ESS/ESS-ansokan/Kompletteringar/SSM2012-131-70 Activation studies on ESS target concepts - Draft.pdf](http://www.stralsakerhetsmyndigheten.se/Global/ESS/ESS-ansokan/Kompletteringar/SSM2012-131-70%20Activation%20studies%20on%20ESS%20target%20concepts%20-%20Draft.pdf) 582266\_1\_1.pdf.
- [12] M. U. Khandaker, M. S. Uddin, K. S. Kim, M. W. Lee, Y. S. Lee and G. N. Kim, *Nucl. Instr. Meth. Phys. Res. B* 266 (2008), pp. 1021-1029.
- [13] P. P. Dimitriev and G.A. Molin, *Atom. Energy* 48 (1980), pp.122-130.
- [14] M. Nandy and Sunil C, *Radioactive Waste*, Chapter 6, Intech Open Access Book ISBN 978-953-51-0551-0 (2012).
- [15] M. Nandy and C. Lahiri, *Ind. Jour. Pure & Appl. Phys.* 50 (2012), pp. 761-765.
- [16] K. Tsujimoto, T. Sasa, K. Nishihara, T. Takizuka, H. Takano, K. Hirota and Y. Kamishima, 7<sup>th</sup> Int. Conference on Nuclear Engineering, Tokyo, Japan, *ICONE-7092* (1999).